Journal of Korean Association of Crystal Growth
Vol. 7, No. 1 (1997) 59-69

Epitaxial growth and microstructural characterization of YSi_2 films on (100)Si substrate

Young-Ki Lee
Department of Electronic Materials Engineering, Ui-Duk University, Kyungju 780-910, Korea

이트리움 실리사이드 박막의 (100)Si 기판상에서의 방향성 성장과 미세조직의 특성

이영기
위덕대학교 전자재료공학과, 경주, 780-910

Abstract The growth and microstructural characterization of epitaxial yttrium silicide (YSi_2) on the (100)Si substrate are investigated. The YSi_2 film grow epitaxilly through the solid phase reaction during vacuum annealing above 400℃. The epitaxial relationships between the hexagonal YSi_2 film and the (100)Si substrate are $[0001]YSi_2 /\!/ [01\bar{1}]Si$ and $[0001]YSi_2 /\!/ [0\bar{1}\bar{1}]Si$ in the $(1\bar{1}00)YSi_2 /\!/ (100)Si$ plane relation. The YSi_2 film consists of the two types of domains which have two different azimuthal orientations making an angle of 90° to each other. The two types of domains in the YSi_2 film are equivalent in volume fraction and crystalline quality, which has been proved from the equivalent integrated intensities of $(2\bar{2}0\bar{1})$ asymmetric reflection of X-ray diffraction. The formation of a double-domain structure is discussed on the basis of geometrical matching at interface between the $(1\bar{1}00)YSi_2$ film and the (100)Si substrate, and growth model is proposed.

요 약 이트리움 실리사이드(YSi_2)는 400℃ 이상의 진공열처리 중 고상반응에 의하여 (100)Si 기판상에서 YSi_2의 $(1\bar{1}00)$면이 방향성 성장을 하였으며, YSi_2 박막과 (100)Si 기판과의 방위관계는 $[0001]YSi_2 /\!/ [01\bar{1}]Si$과 $[0001]YSi_2 /\!/ [0\bar{1}\bar{1}]Si$이었다. 그러나 방위관계에서도 알 수 있는 바와 같이 YSi_2는 $(1\bar{1}00)YSi_2$의 domain이 상호간에 90°의 방위각을 이루며 성장하는 이른바 double-domain 구조를 나타내었다. 이는 $(1\bar{1}00)YSi_2$면과 Si기판과의 계면에서 커다란

격자 불일치의 이방성 때문이라 생각되며, 각각의 domain은 $(2\bar{2}0\bar{1})$ 비대칭 반사면의 ω-mode rocking curve 측정 결과, 거의 동등한 체적율과 결정성을 나타내었다. 본 연구에서는 이러한 double-domain의 형성기구를 $(1\bar{1}00)YSi_2$면과 (100)Si기판과의 계면에서 정합 모델에 근거한 기하학적 matching 관계로 설명하였다.

1. Introduction

Thin silicide films formed through solid phase reaction of evaporated metal layers with the silicon substrates have received wide attention beause of the technical importance for ohmic and Schottky contacts in silicon-based semiconductor devices [1-5]. Among these silicides, some rare-earth (RE) silicides have been especially attractive over the last few years. They form contacts with the lowest Schottky barrier height (Φ_B : 0.3~0.4 eV) on n-type silicon among the studied silicides, and therefore they can be used as ohmic contacts in silicon devices [6,7]. Furthermore, interest in the epitaxial RE silicides has increased considerably in the recent years, for the fundamental studies of the interface [8,9].

RE silicides crystallize in a hexagonal AlB_2 structure with the space group P6/mmm [10,11]. They are nearly lattice-matched in the growth of their (001) planes on the (111)Si surface : the lattice mismatch varies from nil for yttrium silicide (YSi_2) to -2.55 % for lutetium silicide ($LuSi_2$) at room temperature. Thus, under ideal conditions, the triangular atomic arrangement of the RE silicide layers would match up to the 3-fold symmetric (111)Si plane. The YSi_2 has been extensively investigated, and the $(0001)YSi_2$ layer has been found to grow on the (111)Si substrate with highly-perfected orientation through solid phase reaction [8,9]. Alth-ough (100)Si substrates have been used in most of the practical silicon devices, very little work for the epitaxial growth of RE silicides on (100)Si substrates has been done [12,13] and furthermore their detailed crystallographic analysis have not yet been described.

In this study, the solid phase epitaxy of the YSi_2 formed during vacuum furnace annealing is investigated. The epitaxial relationship and the occurrence of double domains are shown experimentally, and the epitaxial growth mode is discussed on the basic of geometrical matching at the interface between the yttrium silicide and the (100)Si substrate.

2. Experimental details

The substrates were p-typed (100)Si wafers of 2 inch diameter with resistivity of about 10 Ω·cm. Prior to the deposition of the Y layer, the Si surface was cleaned with organic solvents, rinsed in distilled water, followed by immersion in dilute hydrofluoric acid to remove the native oxide layer, and finally rinsed in distilled water and dried with

dry nitrogen. After these cleaning steps, the wafer was immediately loaded into a vacuum chamber, which was kept at a pressure below 5×10^{-6} Torr during deposition. In order to reduce the amount of gaseous impurities incorporated in the source metal, the Y source (99.9 %) was outgassed before deposition. The Y layer of 1000 Å thickness was deposited onto the cleaned wafer by an electron beam evaporation method without heating of the substrate. The deposition rate of the Y layer was 10 Å/s. Subsequently, a thin Si layer of 500 Å thickness was additionally deposited on the Y film without breaking of the vacuum in the same chamber to prevent the Y film from oxidation during handling, because Y oxidizes very quickly in air even at room temperature. The deposition rate of Si layer was 40~50 Å/s. The deposition rates of Y and Si were monitored with a resonator plate of a quartz crystal, and the thickness was determined with a surface profilometer after deposition.

The as-deposited sample was cut into several pieces, and each of them was annealed in vacuum for the growth of an yttrium silicide layer. The vacuum annealing system was composed of a furnace and silica tube which was evacuated at a pressure below 6×10^{-7} Torr. The samples were annealed at temperatures of 300 to 900℃ for various times, ranging from 10 to 300 min.

Transmission electron microscopy (TEM) and selected area diffraction (SAD) were applied to characterize the microstructure and to determine the orientation relationships between the grown silicide layer and the (100)Si substrate. TEM samples were prepared by ultrasonic cutting to 3 mm diameter and thinning from the silicon side with mechanical polishing and chemical etching ($HF : HNO_3 = 1 : 1$). The crystallographic characterization of the YSi_2 surface was evaluated by reflection high-energy electron diffracton (RHEED). X-ray diffraction (XRD) was used to identify the cry stalline phases formed by annealing. The ω-mode rocking curves were also measured to determine the volume fractions of the two domains rotated by 90° around the common $[1\bar{1}00]YSi_2$ axis in the silicide film. For the crystallographic characterization, the full width at half-maximum (FWHM) of the diffraction curve was examined.

3. Results and discussion

The formation of silicide phases in the reacted layers was investigated by XRD using CuK_α radiation. Figure 1 shows the typical XRD pattern from the sample annealed at 600℃ for 60 min. Above the growth temperature of silicide (400℃), the hexagonal YSi_2 phase becomes detectable with the presence of strong $(1\bar{1}00)$ and $(2\bar{2}00)$ diffraction peaks, except for peaks from the Si substrate and from the Y_2O_3. The absence of other allowed YSi_2 peaks, especially the $(10\bar{1}1)$ peak ($2\theta = 35.02°$) which is about 2.5 times more intense than the $(1\bar{1}00)$ peak in the YSi_2 powder diffraction data [14], surely indicates that the YSi_2 film has a preferred orientation. The $(1\bar{1}00)$ plane of the

YSi_2 is parallel to the (100)Si surface, that is, with its a-and c-axes lying on the (100) Si plane. The diffraction patterns of numerous samples annealed above 400℃ have been quite similar to those of Fig. 1, except that the intensities of the YSi_2 diffraction peaks become stronger, and the peak corresponding to Y_2O_3 [15] becomes weak with an increase of annealing temperature and time. Futhermore, the Y_2O_3 peak has almost never been detectable after annealing above 900℃, although not shown here. It is considered that the annealing at higher temperature may serve to drive off oxygen from the silicide film, because the annealing leads to the dissolution of the Y oxide. A similar behavior of oxygen has been observed during the formation of RE silicides at higher temperatures [16,17].

The crystallographic orientation of the YSi_2 film is examined in detail by RHEED. Figure 2a shows the RHEED pattern obtained from an YSi_2 film after annealing at 900℃ for 60 min. The spotty pattern from

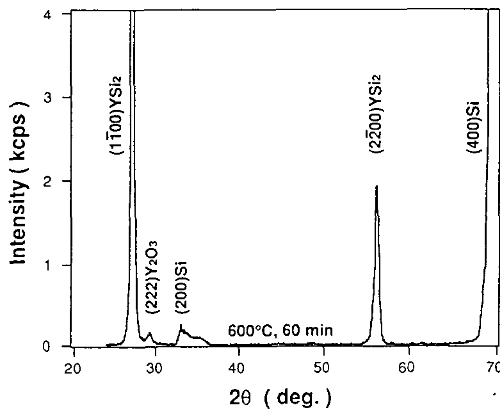

Fig. 1. XRD patterns from the Si/Y/(100)Si samples annealed at 600℃ for 60 min.

YSi_2 and the dim ring pattern from Y_2O_3 phase is observed. The patterns of reciprocal lattice points for the [11$\bar{2}$0] and [0001] azimuthal incidences on the (1$\bar{1}$00)YSi_2 single crystal are also shown in Figs. 2b and 2c, respectively. The RHEED pattern of YSi_2 in Fig. 2a includes spots from the [0001]YSi_2 incidence and from the [11$\bar{2}$0]YSi_2 incidence, i.e., the pattern in Fig. 2a is accordant with the intermixing of patterns of Figs. 2b and 2c. The [11$\bar{2}$0] and [0001] incidences are perpendicular to each other. There are no change in the RHEED pattern observed by rotating the sample by 90°. This

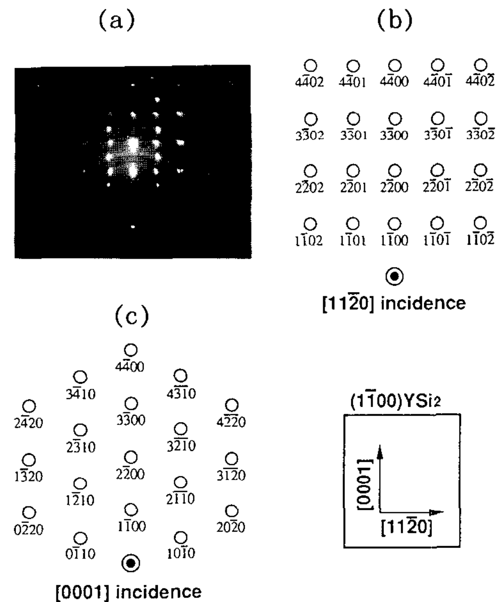

Fig. 2. (a) RHEED pattern from the (1$\bar{1}$00) YSi_2 film grown by vacuum annealing at 900℃ for 60 min. (b), (c) patterns of reciprocal lattice points for the [11$\bar{2}$0] and [0001] azimuths, respectively. Note that the angle between [11$\bar{2}$0] and [0001] incident directions is 90°

fact shows that the (1$\bar{1}$00)YSi_2 film has grown on the (100)Si in the form of the double-domain structure, in which the azimuthal angle between the two domains is 90° and these two kinds of domains are distributed throughout the film.

The microstructure and the orientation relationship of the YSi_2 film have been investigated by TEM(JEM-2000FX) operated at 200 kV. Most of TEM micrographs were taken by the incidence along the [100] zone axis of single-crystal Si substrate. In as-deposited state, the yttrium layer consists of randomly oriented Y grains with the diameter of 100-400 Å without the formation of any other phases. However, the hexagonal YSi_2 begins to grow epitaxially by annealing above 400℃ for 10 min. Figure 3a is the SAD pattern from the YSi_2/(100)Si specimen annealed at 600℃ for 60 min, and Fig. 3b the schematic patterns. When comparing Fig. 3a with Fig. 3b, it is confirmed that there are two domains of (1$\bar{1}$00)YSi_2 on (100)Si which have azimuthal orientations perpendicular to each other in the plane, although double diffraction leads to a complex array of diffraction spots in this pattern. The orientation reltionships (ORs) between the thin film and the substrate can be deduced from Fig. 3 as follows :

[0001]YSi_2 // [01$\bar{1}$]Si in (1$\bar{1}$00)YSi_2 // (100)Si : OR_1,
[0001]YSi_2 // [0$\bar{1}\bar{1}$]Si in (1$\bar{1}$00)YSi_2 // (100)Si : OR_2,

On the geometrical symmetry at the interface, OR_1 and OR_2 are exactly equivalent; both are obtained by rotating the other by 90° around the common [1$\bar{1}$00]YSi_2 axis.

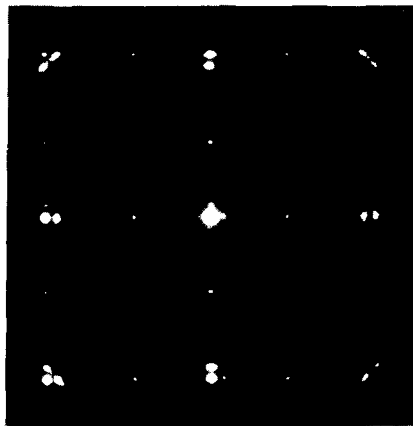

(a)

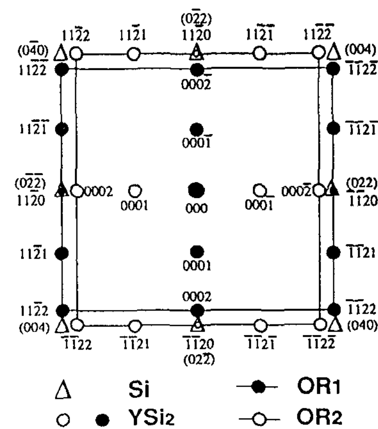

(b)

Fig. 3. (a) SAD pattern from the (1$\bar{1}$00)YSi_2 film grown by vacuum annealing at 600℃ for 60 min. (b) Schematic pattern of (a) showing the (1$\bar{1}$00)YSi_2 // (100)Si epitaxy. The open triangles denote reciprocal lattice points of (100)Si, and the closed and open circles denote those of OR_1 and OR_2 of (1$\bar{1}$00)YSi_2 film, respectively.

This suggests that the $(1\bar{1}00)YSi_2$ film consists of a double-domain structure having two different azimuthal orientations throughout the film, as shown in Fig. 2.

Also, the fact that the $(1\bar{1}00)YSi_2$ film consists of a double-domain structure can obviously be recognized from the microstructure observation by TEM. Figure 4 shows a bright-field image of TEM taken from the region corresponding to the SAD pattern of Fig. 3. The parallel moiré patterns or fringes in domains provide some valuable information on the relaxation of the misfit strain. These moiré patterns or fringes normal to the c-axis of YSi_2, observed owing to double diffraction between YSi_2 and Si layer, reveal an average spacing of about 52 Å. The predicted parallel moiré fringe spacings are 52.4 Å for a lattice mismatch of 7.9 % between the $(0001)YSi_2$ and the (001)Si. Hence it is clear that the strain has been relieved by the creation of misfit dislocations

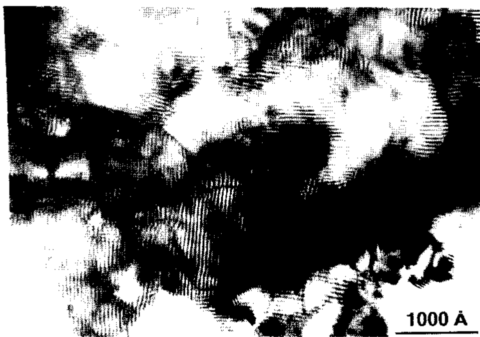

Fig. 4. Bright-field image from the (1100) YSi_2 film grown by vacuum annealing at 600℃ for 60 min. Note that the parallel moiré fringes for the two different types of domains are perpendicular to each other.

at the interface between each domain and substrate. The domains of about 700 Å in diameter and domain boundaries were observed. At these domain boundaries, the moiré fringes are discontinuous and irregular in their shapes. Two perpendicular orientations in individual domains with the same moiré fringe spacing were also found. This means that each epitaxial domain tends to take two different azimuthal orientations rotated by 90°, as exhibited in the SAD pattern of Fig. 3.

Figure 5 shows a HRTEM (highresolution TEM) image for only YSi_2 film taken from the same sample shown in Fig. 3, which can distinctly observe the domain boundaries and lattice image. The interp-laner spacings measured in Fig. 5 are about 4.1 Å. This corresponds to the (0001) lattice spacing (4.144 Å in Ref. 14) of YSi_2, which indicates that the c-axis of YSi_2 is parallel to the (100)Si substrate surface. The lattice images for two domains designated as A, B in Fig. 5 are perpendicular to each other. Therefore, it is obvious that the $(1\bar{1}00)YSi_2$ film consists of the double-domain structure.

To determine the volume fractions of the two kinds of domains making an angle of 90° around the common $[1\bar{1}00]YSi_2$ axis, it was measured the X-ray integrated intensities of $(2\bar{2}0\bar{1})$ asymmetric reflection. Figure 6 shows an outline of the stereographic projection of $(1\bar{1}00)YSi_2$ including the two types of domains, OR_1 (closed circles) and OR_2 (open circles), and the orientation of (100)Si. Although the X-ray diffraction in-

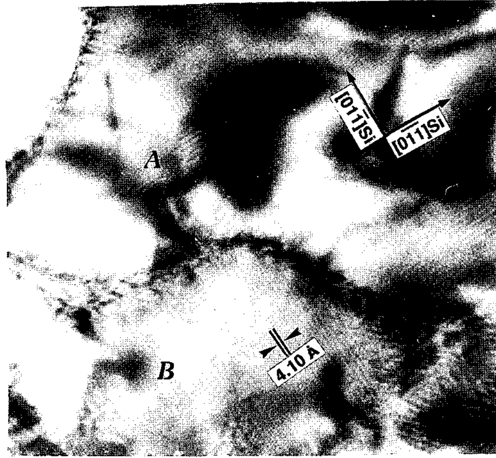

Fig. 5. HRTEM image from the only YSi_2 film grown by vacuum annealing at 900℃ for 60 min. The interplanar spacing is about 4.1 Å, and this corresponds to the (0001) lattice spacing of YSi_2 crystal. Note that the lattice fringes within two domains (A and B) are perpendicular to each other.

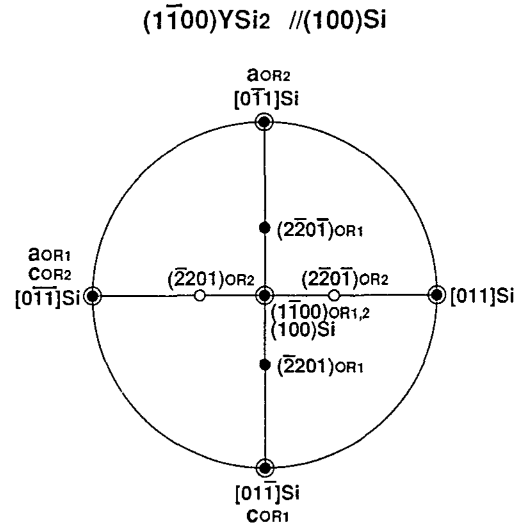

Fig. 6. An outline of the stereographic projection of $(1\bar{1}00)YSi_2$ including the two types of domains, OR_1 (closed circles) and OR_2 (open circles), and the orientation of (100)Si.

tensity of symmetric reflections such as $(1\bar{1}00)$ and $(2\bar{2}00)$ planes contains that of reflection from OR_1 and OR_2 together, the observation of asymmetric reflection such as $(2\bar{2}0\bar{1})$ reflection enables us to obtain the diffraction intensity from each of the two types of domains. The OR_1 is observed by $(2\bar{2}0\bar{1})$ reflection with the $[01\bar{1}]$Si azimuth in the plane of X-ray incidence and the OR_2 with the $[0\bar{1}\bar{1}]$Si azimuth in the plane. Therefore, it can be obtained the volume fractions of the two types of domains on comparing the two integrated intensities in the X-ray rocking curves.

Figure 7 shows ω-mode rocking curves for the $(2\bar{2}0\bar{1})$ asymmetric reflection of OR_1 (a) and OR_2 (b) in the $(1\bar{1}00)$ YSi_2 film grown on the (100)Si substrate by annealing at 600℃ for 60 min. The respective curves are obtained separately by the measurements before and after rotating of the sample by 90° around the $[1\bar{1}00]$ axis, as shown in Fig. 5. The reflection arrangements are schematically shown by the inserted figures in Fig. 7. The integrated intensities as well as the rocking curves are almost identical for the OR_1 and OR_2. This fact means that the volume fractions of the OR_1 and the OR_2 are equal to each other in the $(1\bar{1}00)YSi_2$ film since a direct comparison of the integrated intensities obtained from the two types of domains gives their volume fractions. The FWHMs of two rocking curves are almost similar values, that is ,

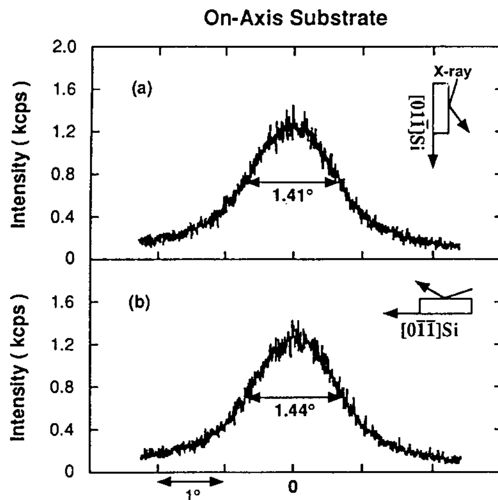

Fig. 7. Rocking curves of the $(2\bar{2}0\bar{1})$ asymmetric reflection for OR_1 (a) and OR_2 (b) in the $(1\bar{1}00)YSi_2$ film grown by vacuum annealing at 600℃ for 60 min. Note that intensities for (a) and (b) are almost identical.

0.84° for OR_1 and 0.86° for OR_2. This implies that the crystalline quality of the OR_1 and the OR_2 is exactly equivalent, because the FWHM of a diffraction curve is the indicative of the crystalline quality.

In the heteroepitaxy of two materials with different crystal structures, an exact geometrical matching is nearly impossible. It is therefore, expected that a good two-dimensional matching at the interface is necessary for the origination of an epitaxial growth mode in a given deposit/substrate system, even though the chemical interatomic interactions at the interface may play an important role [18-20]. The heteroepitaxial growth of YSi_2 layers on the 4-fold symmetric (100)Si can be deduced from the geometrical matching at the interface between the $(1\bar{1}00)YSi_2$ and the (100)Si substrate. From the observations of SAD and RHEED patterns, it represents the schematic top view of the atomic arrangement in the epitaxial relation between YSi_2 and Si, as shown in Fig. 8. The YSi_2 has a hexagonal structure based on the AlB_2 structure, with lattice parameters $a_0=3.842$ Å and $c_0=4.144$ Å [14], while the d-spacing of (110)Si is 3.840 Å [21]. Thus, the interface in the heteroepitaxial $(1\bar{1}00)YSi_2/\!/(100)Si$ system has large anisotropy in lattice mismatch : 7.9 % for the $[0001]YSi_2$ direction and 0.05 % for the $[11\bar{2}0]YSi_2$, at room temperature. As a result, it is considered that there are two possible ways for the epitaxial growth of $(1\bar{1}00)YSi_2$ with 2-fold symmetry on (100)Si with 4-fold symmetry as denoted with OR_1 and OR_2 in Fig. 8 : (i) the growth toward the $[01\bar{1}]$Si, OR_1 (ii) the growth toward the $[0\bar{1}\bar{1}]$Si, OR_2. The strains per area are expected to be identical for these arrangements. A physical explanation for the appearance of the double-domain structure in this epitaxial layer can be related to growth procedures and crystallization of the silicide.

Generally, thin films are formed on a substrate through a process of nucleation and growth. The epitaxy of a continuous film may be determined by a combination of them : (i) oriented nucleation during the formation of small clusters, (ii) reorientation during coalescence stage, and (iii) reorientation (regrowth) of large crystallites [22]. In this $(1\bar{1}00)YSi_2/\!/(100)Si$ system, the epitaxy can be considered by oriented

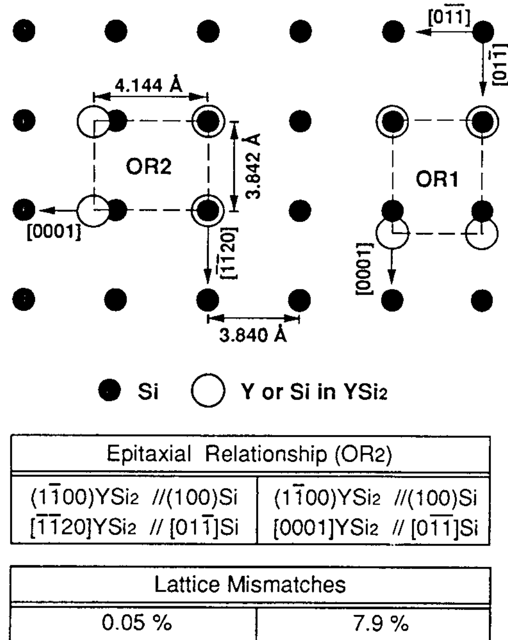

Epitaxial Relationship (OR2)	
$(1\bar{1}00)YSi_2$ //(100)Si $[\bar{1}\bar{1}20]YSi_2$ // $[01\bar{1}]$Si	$(1\bar{1}00)YSi_2$ //(100)Si $[0001]YSi_2$ // $[0\bar{1}\bar{1}]$Si

Lattice Mismatches	
0.05 %	7.9 %

Fig. 8. A schematic top view of the heteroepitaxial $(1\bar{1}00)YSi_2$∥(100)Si system, the epitaxial relationships, and the lattice mismatches.

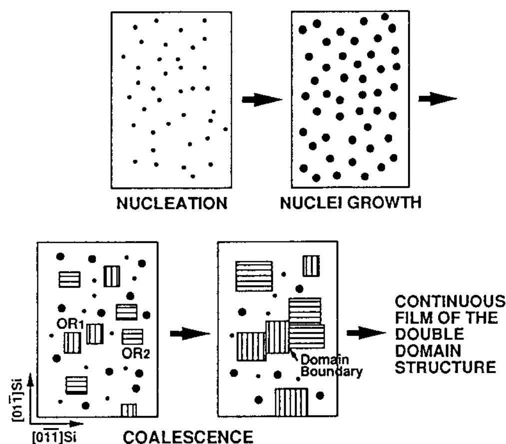

Fig. 9. Schematic stages for the double-domain growth of $(1\bar{1}00)YSi_2$ film in the heteroepitaxial $(1\bar{1}00)YSi_2$∥(100)Si system.

nucleation during the formation of small clusters, and the epitaxial steps are shown schematically in Fig. 9. Baglin et al. have reported that the RE silicides nucleate in a few spot during the initial stage and then grow as isolated islands through Volmer-Weber growth (three-dimensional growth) process during a solid-phase reaction [10-23]. During the initial stage of nucleation of the silicide, therefore, the interfacial energy for the growth of OR_1 and OR_2 are identical because two directions are equivalent on the surface of (100)Si, and the formation probability of discrete three-dimensional nuclei of OR_1 and OR_2 domains is also equal. Firstly, by furnace annealing above 400℃, Si atoms diffuse into Y layer to form cluster. When clusters reach a certain critical size they become stable entities, called nuclei. Subsequently, once nucleated, film growth proceeds predominantly by the growth of nuclei and their eventual coalescence stage as follows : the large nuclei grow larger with the expense of the small ones. During the coalescence stage of the $(1\bar{1}00)YSi_2$ nuclei, if a critical sized nucleus (OR_2) is contiguous to a critical sized nucleus with same orientation (OR_2), respective nuclei can be grown as an identical domain (OR_2). On the other hand, if the initial nuclei with two different orientations are contiguous, i.e., OR_1 and OR_2, respective nuclei can be grown as two types of domains which have two different azimuthal orientations making an angle of 90° to each other. The above growth steps are shown schematically in Fig. 9. As a result, the volume fraction and the crystal-

line quality of two domains with OR_1 and OR_2 are considered to be identical in to $(1\bar{1}00)YSi_2$ film. These facts has been explicitly shown in this experimental result of Fig. 7. However, more detailed microscopic study using TEM, especially during the initial silicidation, will be needed to clarify the formation mechanism of a double-domain $(1\bar{1}00)YSi_2$ film grown on (100)Si substrate through a solid phase reaction.

4. Conclusions

The epitaxial growth of YSi_2 on (100)Si substrate is established through a solid phase reaction during vacuum annealing above 400℃. The thin film of the hexagonal YSi_2 has a preferred matching face relationship on (100)Si, $(1\bar{1}00)YSi_2$ // (100)Si. However, the $(1\bar{1}00)YSi_2$ film is not single crystal. This consists of two types of domains having two different azimuthal orientations, [0001] and $[11\bar{2}0]$ orientations along the $[0\bar{1}\bar{1}]$ orientation on (100)Si, which make an angle of 90° to each other around the common $[1\bar{1}00]YSi_2$ axis. The domain size is about 700 Å. The volume fractions of the two types of domains with OR_1 and OR_2 are identical, and their crystalline quality is exactly equivalent.

For the heteroepitaxial $(1\bar{1}00)YSi_2$ // (100)Si system, there is an anisotropy in lattice mismatch at the interface. The strains induced by the lattice mismatch are relieved by the creation of misfit dislocations at the interface between domain and substrate. The respective interfacial energy for the growth of $(1\bar{1}00)YSi_2$ toward the $[01\bar{1}]$Si and toward the $[0\bar{1}\bar{1}]$Si are identical during the initial stage of epitaxial growth of the silicide. As a result, the two types of domains with OR_1 and OR_2 in the YSi_2 film become equivalent in volume fraction and crystalline quality.

References

[1] S.P. Muraka, J. Vacuum Sci. Technol. 17(1980) 775.

[2] F.M. d'Heurle, C.S. Peterson and M.Y. Tsai, J. Appl. Phys. 51 (1980) 5976.

[3] J.W. Mayer and K.N. Tu, J. Vacuum Sci. Technol. 11 (1974) 86.

[4] G.A. Huchins and A. Shepara, Thin Solid Films 18 (1973) 343.

[5] R.W. Bower and J.W. Mayer, Appl. Phys. Lett. 20 (1972) 359.

[6] K.N. Tu, R.D. Thomson and B.Y. Tsaur, Appl. Phys. Lett. 38(1981) 626.

[7] H. Norda, J. de Sousa Pires, F.M. d'Heurle, F. Pesavento, C.S. Peterson and P.A. Tove, Appl. Phys. Lett. 38 (1981) 865.

[8] F.A. d'Avitaya, A. Perio, J.C. Oberlin, Y. Campidelli and J.A. Chroboczek, Appl. Phys. Lett. 54 (1989) 2198.

[9] J.A. Knapp and S.T. Picraux, Mater. Res. Soc. Symp. Proc. 54 (1986) 261.

[10] J.E.E. Baglin, F.M. d'Heurle and C.S. Peterson, J. Appl. Phys. 52 (1981) 2481.

[11] A. Iandelli, A. Palenzona and G.L.

Olcese, J. Less-Comm. Mat. 64 (1979) 213.

[12] Y.K. Lee, N. Fujimura and T. Ito, J. Alloys & Compounds 193 (1993) 289.

[13] A. Travlos, P. Aloupogiannis, E. Rokofyllou, C. Papastaikoudis, G. Weber and A. Traverse, J. Appl. Phys. 72 (1992) 948.

[14] Standard X-Ray Diffraction Pattern, File No. 11-596.

[15] Standard X-Ray Diffraction Pattern, File No. 25-1200.

[16] M. Gurvitch, A.F.J. Levi, R.T.Tung and S. Nakahara, Appl. Phys. Lett. 51 (1987) 311.

[17] C.S. Wu, D.M. Scott and S.S. Lau, J. Appl. Phys. 58 (1985) 1330.

[18] A. Zur and T.C. McGill, J. Appl. Phys. 55 (1984) 378.

[19] L.A. Bruce and H. Jaegar, Phil. Mag. A 37 (1978) 337.

[20] K. Takayanagi, K. Yaki and G. Honjo, Thin Solid Films 48 (1978) 137.

[21] Standard X-Ray Diffraction Pattern, File No. 27-1402.

[22] R. Ludeke, J. Vacuum Sci. Technol. B 2 (1984) 400.

[23] J.E.E. Baglin, F.M. d'Heurle and C.S. Peterson, Appl. Phys. Lett. 36 (1980) 594.